

FEDSM-ICNMM2010-' 0% \$

DEPENDENCE OF THE CONTACT ANGLE ON ADSORPTION AT THE SOLID-LIQUID INTERFACE

C. A. Ward*

Thermodynamics and Kinetics Laboratory
Department of Mechanical and Industrial Engineering
University of Toronto
Toronto, Ontario, M5S 3G8
CANADA
Email: charles.ward@utoronto.ca

ABSTRACT

A method for determining the surface tension of solid-fluid interfaces has been proposed. For a given temperature and fluid-solid combination, these surface tensions are expressed in terms of material properties that can be determined by measuring the amount of vapor adsorbed on the solid surface as a function of x^V , the ratio of the vapor-phase pressure to the saturation-vapor pressure. The thermodynamic concept of pressure is shown to be in conflict with that of continuum mechanics, but is supported experimentally. This approach leads to the prediction that the contact angle, θ , can only exist in a narrow pressure range and that in this pressure range, the solid-vapor surface tension is constant and equal to the surface tension of the liquid-vapor interface, γ^{LV} . The surface tension of the solid-liquid interface, γ^{SL} , may be expressed in terms of measurable properties, γ^{LV} and θ : $\gamma^{SL} = \gamma^{LV}(1 - \cos \theta)$. The value of θ is predicted to depend on both the pressure in the liquid at the three-phase, line x_3^L , and the three-phase line curvature, C_{cl} . We examine these predictions using sessile water droplets on a polished Cu surface, maintained in a closed, constant volume, isothermal container. The value of θ is found to depend on the adsorption at the solid-liquid interface, $n^{SL} = n^{SL}(x_3^L, C_{cl})$. The predicted value of θ is compared with that measured, and found to be in close agreement, but no effect of line tension is found.

INTRODUCTION

Recently a method for determining the surface tension of solid-fluid interfaces was proposed [1]. This method is based on the ζ -adsorption isotherm. It uses this isotherm to establish the values of the material properties of a solid surface that controls the surface tension of the solid, both in the absence of any adsorption, γ^{S0} , and in the presence of an adsorbed vapor, γ^{SV} . There are four parameters in the ζ -adsorption isotherm, denoted M , c , α and ζ . These parameters are determined for a particular vapor-solid combination by comparing the isotherm expression with measurements of the amount of vapor adsorbed as a function of pressure, for a given temperature, T , and determining the values of the parameters that give the best agreement between the measured amount adsorbed and that predicted to be adsorbed [1–3].

One of the essential properties of any isotherm that is to be used in the proposed procedure is that it does not indicate an infinite amount is adsorbed in the limit of the vapor-phase pressure, P^V , approaching the saturation-vapor pressure, $P_s(T)$. The ζ -adsorption isotherm satisfies this condition, but neither the BET [4] nor the FHH [5–7] do. These isotherms indicate an infinite amount is adsorbed in this limit, and thus, could not be used. A second condition is for the isotherm to be valid for the pressure ratio $x^V [\equiv P^V/P_s(T)]$ between zero and one. If these conditions are met, the isotherm may be incorporated into Gibbsian thermodynamics [8] and the expression for $\gamma^{SV}(T)$ predicted as a function of x^V , and the surface tension of the adsorbing fluid

*Address all correspondence to this author.

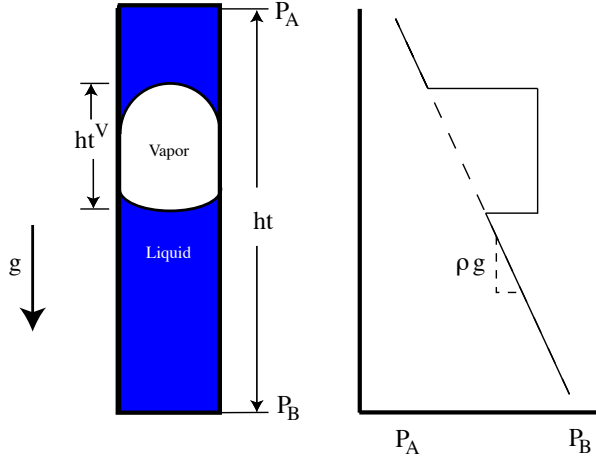


FIGURE 1. The two fluid phases of a substance enclosed in a constant volume, isothermal system along with the predicted pressure profile are shown.

at the liquid-vapor interface, $\gamma^{LV}(T)$.

The theory for determining the surface tension of a solid can then be examined in two limits: in the low pressure limit, the expression for γ^{S0} may be determined from the expression for γ^{SV} by taking the limit of x^V going to zero. Since γ^{S0} is a material property of the solid surface, its value must be the same when determined from the adsorption of different vapors [1, 2]. At pressures where a contact angle of a sessile droplet, θ , can exist, the ζ -isotherm may be employed to predict the value of θ for a sessile droplet enclosed in a constant volume, isothermal container as a function of the number of moles of fluid present [3]. Also, the contact angle in such a system may be measured.

One of the issues raised by these results is the sensitivity of the contact angle to the pressure in the liquid phase at the three-phase line, x_3^V [9, 10]. Thus, it is essential that the pressure is accurately predicted. We show that the idea of pressure in a two-phase fluid being determined by the “weight of the fluid above” [11] does not agree with the thermodynamic concept of pressure: the pressure is such that there is no net molecular transport across a horizontal plane when gravity acts normal to the plane [9, 12].

THE CONDITIONS FOR THERMODYNAMIC EQUILIBRIUM

When Gibbsian thermodynamics [8] is employed to determine the conditions for equilibrium in a system containing the two fluid phases of a substance that is exposed to a gravity field of intensity, g , such as that shown in Fig. 1, one obtains three conditions.

1. If W denotes the molecular weight of the fluid, the gravity field is $-g\mathbf{i}_z$, the chemical potentials in the liquid and va-

por phases, $\mu^L[T, P(z)]$ and $\mu^V[T, P(z)]$, respectively must be such that there is no net molecular transport across any horizontal plane in the fluid that is perpendicular to the direction of the gravity vector. If j is equal L or V, then

$$\mu^j + Wgz = C_j, \quad (1)$$

where C_j is a constant.

2. The pressure in the liquid and vapor phases at the liquid-vapor interface, $P_l^L(z)$ and $P_l^V(z)$, must satisfy the Laplace equation

$$P_l^V(z) - P_l^L(z) = \gamma^{LV}(C_1^{LV} + C_2^{LV}), \quad (2)$$

where C_1^{LV} and C_2^{LV} are the interface curvatures.

3. If the droplet is axisymmetric with the three-phase line curvature C_{cl} and the liquid-phase pressure ratio there is x_3^L , the Young equation gives:

$$\gamma^{SV} - \gamma^{SL} = \gamma^{LV} \cos \theta(C_{cl}, P_3^L). \quad (3)$$

where we have neglected any effect due to line tension [13].

As these relations stand, they do not form a closed set, but they may be closed by adding three equations of state. We approximate the vapor as an ideal gas, the liquid as incompressible, and introduce the ζ -isotherm to describe the amount adsorbed at the solid-vapor interface, n^{SV} . This adsorption isotherm approximates the adsorbed vapor as a collection of molecular clusters, with the clusters consisting of different numbers of molecules, up to a maximum of ζ in a cluster [1]. The isotherm expression is

$$n^{SV} = \frac{Mc\alpha x^V [1 - (1 + \zeta)(\alpha x^V)^\zeta + \zeta(\alpha x^V)^{1+\zeta}]}{(1 - \alpha x^V)[1 + (c - 1)\alpha x^V - c(\alpha x^V)^{1+\zeta}]}, \quad (4)$$

where c and α are temperature dependent parameters that are to be determined along with M and ζ from measurements of the amount adsorbed as a function of x^V . When a sessile droplet is present, the pressure is very near $P_s(T)$, and as seen in Fig. 2, the amount adsorbed is very sensitive to pressure, for pressure ratios near unity.

From the Gibbs adsorption equation at the solid-vapor interface and the expression for n^{SV} , the expression for γ^{SV} may be constructed in terms of the isotherm parameters. One finds [1]

$$\gamma^{SV}(x^V) = \gamma^{LV} - Mk_b T \ln \left(\frac{(\alpha - 1)[1 + (c - 1)\alpha x^V]}{(\alpha x^V - 1)[1 + (c - 1)\alpha]} \right), \quad (5)$$

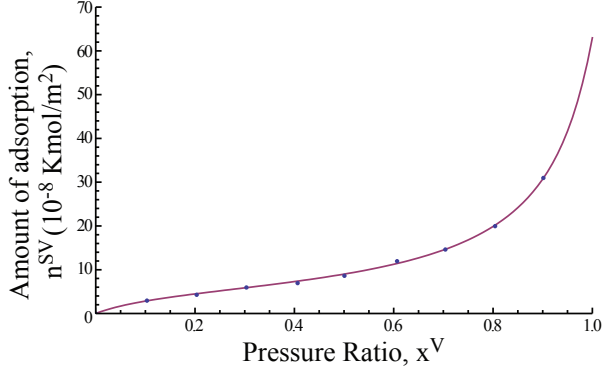


FIGURE 2. The measured amount of water vapor adsorbing on copper at 30 °C [14]. The solid line is the amount calculated to be adsorbed when ζ , α , c and M are assigned values of 60, 0.914, 8.59 and 5.556×10^{-8} kmol/m² respectively.

where we have adopted the wetting hypothesis. This hypothesis assumes that in the limit of θ approaching zero, the surface tension at the solid-liquid interface, γ^{SL} , also goes to zero. The Young Eq., (3) indicates γ^{SV} is equal to γ^{LV} of the adsorbing fluid in this limit.

THE PRESSURE PROFILE IN A TWO-PHASE SYSTEM

We first examine the predicted pressure as a function of height that is obtained from the conditions for equilibrium for a system such as that shown in Fig. 1. If Eq. (1) is applied at two points in the liquid phase, say z_1^L and z_2^L where $z_1^L > z_2^L$, then

$$\begin{aligned} \mu^L[T, P_s(T)] + v_f[P^L(z_1) - P_s(T)] + \\ Wgz_1 = \mu^L[T, P_s(T)] + \\ v_f[P^L(z_2) - P_s(T)] + Wgz_2, \end{aligned} \quad (6)$$

where v_f denotes the molar specific volume of the liquid at saturation. Thus,

$$P(z_2^L) = P(z_1^L) + \frac{Wg}{v_f}(z_1^L - z_2^L). \quad (7)$$

The predicted pressure profile is shown in Fig. 1 [12]. As seen there, the slope of the pressure in the liquid phase is predicted to be the same as it would have been had no vapor phase been present. Thus, for the two systems shown in Fig. 3 where the pressure at the top of the cylinder is P_A , both the thermodynamic and continuum mechanics concepts of pressure would predict the same value for the pressure P_C , but they would predict different values of the pressure P_B .

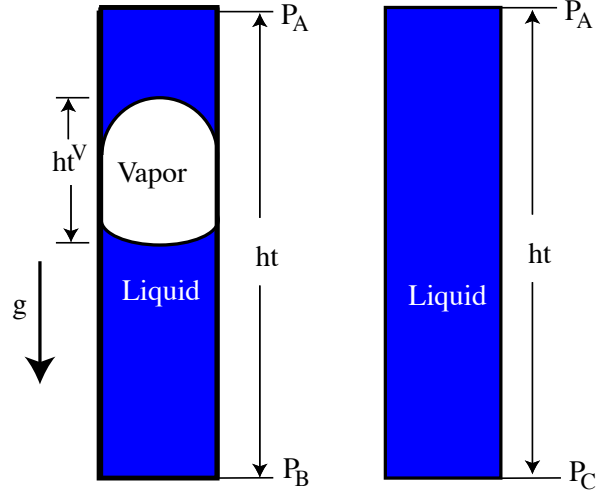


FIGURE 3. According to thermodynamics the pressure P_B is equal to P_C , but according to continuum mechanics $P_C > P_B$ [12].

For the container on the left in Fig. 3, since the weight of the fluid above the bottom of the container is less than the one on the right, continuum mechanics would predict that

$$P_C > P_B. \quad (8)$$

But as indicated in Fig. 1, thermodynamics leads to the prediction that

$$P_C = P_B. \quad (9)$$

This issue has important implications for wetting phenomena and has been examined experimentally [9] using the device shown schematically in Fig. 4. In this device, the pressures at z_A in the two liquid columns have the same value. The relative heights of the mercury columns— z_B compared to z_C —indicate the relative pressures at the bottom of the water columns. In the column on the left, water and its vapor fill the column, but only water is present in the other column. If the thermodynamic concept of pressure is valid, z_B will be equal to z_C when the system comes to equilibrium, but if the concept of pressure, as defined in continuum mechanics, is valid, the equilibrium configuration will be that shown in Fig. 4, $z_B > z_C$.

A series of experiments was conducted in which the length of the vapor phase was different in each case. In one experiment, it was 24.36 mm, and initially, the system configuration corresponded with that shown in Fig. 4: the Hg-column height on the left was 1.22 mm greater than that on the right. The evolution of the difference in the Hg-column heights as the system

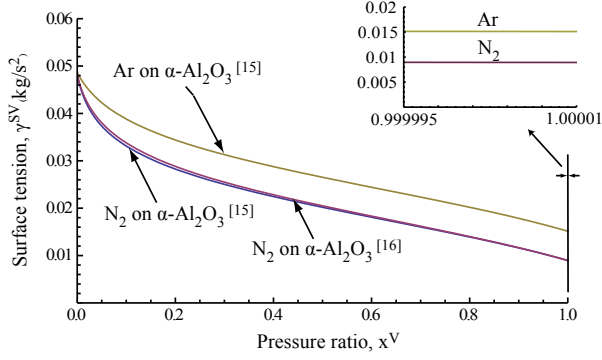


FIGURE 7. The calculated values of γ^{SV} for $\alpha\text{-Al}_2\text{O}_3$ as a function of x^V for two different vapors at 77 K are shown. The adsorption of N_2 was measured in different laboratories [15, 16].

As seen in Fig. 4, as the value of x^V is increased from zero to unity, the predicted effect of the adsorption is to decrease γ^{SV} relative to γ^{S0} , and for a given value of x^V , the amount of decrease depends on the vapor that is adsorbing.

The thickness of the vertical line near x^V equal unity in Fig. 7 indicates the pressure range where the contact angle can exist. The inset figure indicates that in this pressure range, γ^{SV} is reduced to the surface tension of the adsorbing fluid, γ^{LV} . Thus, if x^V approaches unity

$$\gamma^{SV} \rightarrow \gamma^{LV}. \quad (10)$$

Thus, in this pressure range the Young equation, Eq. (3), is predicted to simplify to

$$\gamma^{SL} = \gamma^{LV} [1 - \cos \theta(x_3^L, C_{cl})]. \quad (11)$$

This is an important simplification because both γ^{LV} and θ can be directly measured, and Eq. (11) may be readily applied to determine γ^{SL} . We examine this prediction experimentally below.

Since increasing the pressure in the liquid-phase at the three-phase line has been seen to increase the contact angle (see Fig. 6), Eq. (11) and the results in Fig. 7 indicate the mechanism is adsorption at the solid-liquid interface. But in contrast to the effect of adsorption at the solid-vapor interface, the effect of adsorption at the solid-liquid interface is to increase γ^{SL} . If the adsorption at the solid-liquid interface is denoted n^{SL} and x_3^L is the pressure in the liquid at the three-phase line, the Gibbs adsorption equation at the solid-liquid interface may be written [8, 10, 12]:

$$d\gamma^{SL} = -n^{SL} v_f P_s dx_3^L. \quad (12)$$

For γ^{SL} to increase as x_3^L is increased, Eq. (12) indicates n^{SL} must

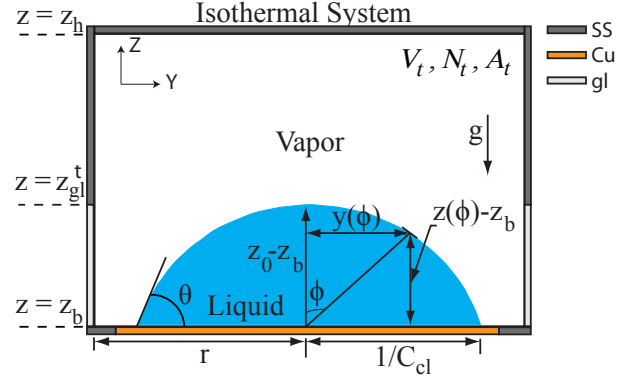


FIGURE 8. Constant volume chamber in which a water droplet could be placed on a polished Cu surface (roughness 53 nm), maintained isothermal at 30 °C, and the number of moles changed.

be negative. The meaning of negative adsorption has been previously investigated and found to mean physically that the fluid concentration within the interphase is less than that in the bulk liquid phase [10].

PREDICTED AND OBSERVED CONTACT ANGLE OF A SESSILE-WATER DROPLET ON A COPPER SUBSTRATE

The low pressure limit of the expression for γ^{SV} given in Eq. (5) is strongly supported by the type of results shown in Fig. 7 [1, 2]. We now want to examine the expressions for γ^{SV} and γ^{SL} , when the pressure is near $P_s(T)$.

For a sessile droplet, there is the possibility of tension existing in the three-phase line [8] that could affect the value of θ . However, estimates of the magnitude of the line tension indicates the actual value of the line tension would have to be several orders of magnitude larger than the theoretical value [13].

Nonetheless, several experimental investigations have indicated that the contact angle depends on the three-phase-line curvature. A recent investigation of the source of this dependence, for a spherical sessile droplet, indicated the source could be adsorption at the solid-liquid interface [17], rather than tension in the three-phase line.

We examined this issue further using sessile water droplets on a copper substrate. Each droplet was enclosed in the apparatus shown schematically in Fig. 8. A droplet could be observed both from above and from the side. The observation from the top allowed the curvature of the three-phase line, C_{cl} , and that from the side allowed the droplet height on the centerline $z_0 - z_b$ to be measured. From these measurements, the conditions for equilibrium may be used to determine both θ and x_0^L . At the

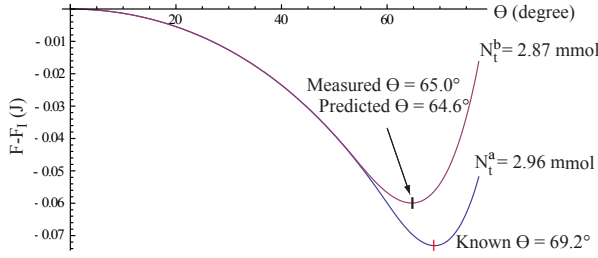


FIGURE 9. The thermodynamic potential for the system is the Helmholtz function. Two calculated Helmholtz functions corresponding to different total numbers of fluid moles are shown. A predicted contact angle corresponds to the minimum in the Helmholtz function.

apex of the axisymmetric droplet

$$\mu^L[T, P^L(z_0)] = \mu^V[T, P^V(z_0)]. \quad (13)$$

Equation (2) may be combined with Eq. (13) to calculate θ , x_0^L , and the curvature of the droplet at the apex, C_0^{LV} [1,2]. We view the contact angle determined in this way as a measurement, since there is little doubt about the validity of the Laplace equation or Eq. (13).

If x_0^L is known, then the pressure at the three-phase line of the droplet may be calculated from Eq. (7):

$$x_3^L = x_0^L + \frac{Wg}{v_f P_s(T)}(z_0 - z_b). \quad (14)$$

The adsorption at the solid-liquid interface may then be obtained from Eqs. (11) and (12)

$$n^{SL} = \frac{\gamma^{LV}}{v_f P_s} \left(\frac{\partial \cos \theta}{\partial x_3^L} \right)_{T, C_{cl}}. \quad (15)$$

A numerical procedure may be used to obtain the value of the partial differential in this equation [2, 10].

The constraints on the system are such that the Helmholtz function acts as the thermodynamic potential. If the contact angle is known, then the number of moles of the fluid component in the system may be determined by determining the condition under which the Helmholtz function is a minimum. This process is illustrated in Fig. 9. In one case, the measured value of the contact angle was 69.2°, but the number of moles in the system was unknown. When the Helmholtz function was plotted for a different number of moles, it was found that the Helmholtz function calculated for 2.96 mmol had a minimum corresponding to the known contact angle, 69.2°.

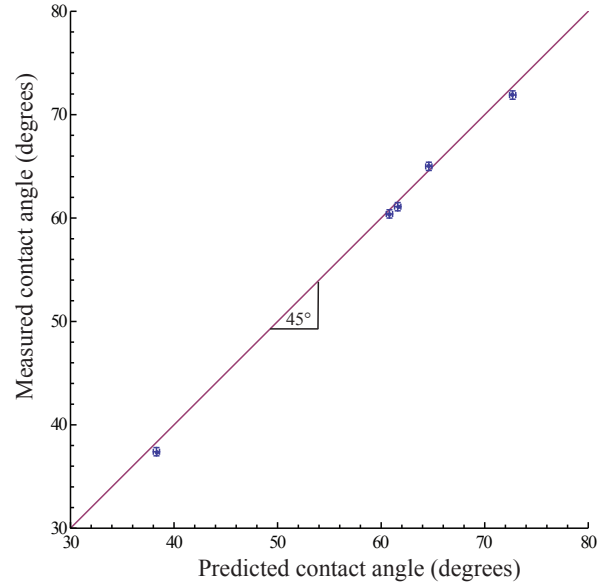


FIGURE 10. The values of the measured and predicted contact angles in a series of experiments are shown.

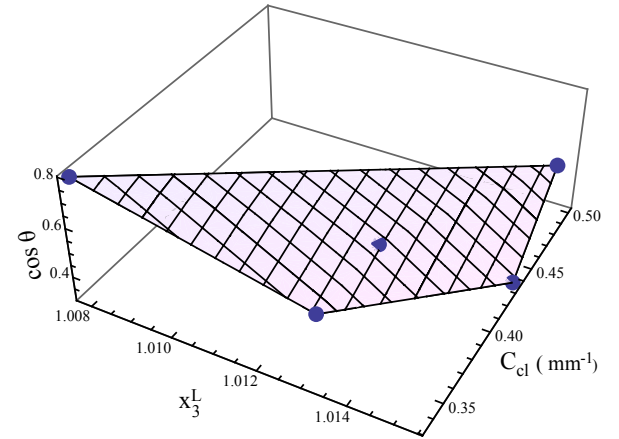


FIGURE 11. Three-dimensional plot of the predicted contact angle as a function of x_3^L and C_{cl} for experiments described in Table 1.

Once the number of moles in the system was known, a vacuum system was used to change the number of moles by a measured amount. For the cases illustrated in Fig. 9, the number of moles was reduced to 2.87 mmol. Then the Helmholtz function could be plotted with the number of moles known, 2.87 mmol. The predicted contact angle was then that corresponding to the minimum in the Helmholtz function, 64.6°. In this second state, the contact angle could also be measured and was 65.0° in this case. In Fig. 10, the measured and predicted values of the contact

TABLE 1. Summary of Experiments with Water Droplets on Cu Conducted at 30 °C [2]

Expt.	$z_0 - z_b$ (mm)	C_{cl} (m ⁻¹)	C_0^{LV} (m ⁻¹)	γ^{LV} (kg/s ²)	x_3^L	γ^{SV} (kg/s ²)	θ (°)	γ^{SL} (kg/s ²)	n^{SL} (mol/m ²)
E1b	0.95 ±0.01	0.333 ±0.006	170.3	0.07119 ±0.000005	1.00777 ±0.00002	0.07112 ±0.002	37.4 ±0.4	0.01456 ±0.0023	-107.427 ±1
E2b	1.19 ±0.01	0.501 ±0.004	373.5	0.07119 ±0.00001	1.01519 ±0.00002	0.07116 ±0.002	61.1 ±0.4	0.03675 ±0.0025	-201.119 ±0.9
E3b	1.58 ±0.01	0.435 ±0.005	354.3	0.07120 ±0.00001	1.01543 ±0.00002	0.07107 ±0.002	71.9 ±0.4	0.04894 ±0.0025	-211.268 ±0.8
E4b	1.38 ±0.01	0.402 ±0.008	295.4	0.07119 ±0.000005	1.01299 ±0.00002	0.07097 ±0.002	60.4 ±0.4	0.0358 ±0.0035	-177.646 ±1
E5b	1.64 ±0.01	0.357 ±0.005	264.6	0.07119 ±0.000005	1.01265 ±0.00002	0.07115 ±0.002	65.0 ±0.4	0.04106 ±0.0025	-178.162 ±0.8

angle obtained using this procedure in a series of experiments are shown (see Table 1). Note the close agreement between the predicted and measured contact angles [3].

Discussion and Conclusion

In Table 1, the results obtained in the sessile-water-droplet experiments are listed. The experimental control variables were the droplet height, $z_0 - z_b$, the curvature of the three-phase line, C_{cl} , and the temperature. These variables were measured in each experiment. From them, the values of x_3^L and θ may be predicted. In Fig. 11, a three-dimensional plot of $\cos \theta$ as a function of x_3^L and C_{cl} is shown, indicating θ has as its independent variables x_3^L and C_{cl} . We emphasize that line tension plays no role in the predicted dependence of θ on C_{cl} .

From the equality of the chemical potentials, x^V may be expressed in terms of x^L

$$x^V(z_b) = \exp\left[\frac{v_f}{v_g}(x^L(z_b) - 1)\right], \quad (16)$$

and one finds that x^V is very near unity. When these values of x^V are used in Eq. (5) to calculate γ^{SV} , one finds the values listed in Table 1. These calculated values of γ^{SV} may be compared with the values γ^{LV} , also listed there. As may be seen in Table 1, they were not measurably different. Thus, Eq. (11) is a valid approximation in all of these experiments [3].

While the surface tension $\gamma^{SV}(x^V)$ was very nearly constant and equal to γ^{LV} , the measured values of θ were between 37.4 and 71.9°. The surface tension γ^{SL} varied by more than a factor of three. Thus, it appears it is the change in γ^{SL} with the experimental variables that is responsible for changing the contact angle.

The mechanism by which γ^{SL} is changed may be investigated by considering the adsorption at the solid-liquid interface. Equation (12) indicates the change in γ^{SL} is proportional to $n^{SL}dx_3^L$. In Fig. 12, we show a plot of n^{SL} as a function of x_3^L and C_{cl} . Note that the dependence of n^{SL} on these variables is very similar to the dependence of $\cos \theta$ on them. This suggests a relation between θ and n^{SL} ; thus, we consider the ratio, λ :

$$\lambda \equiv \frac{\theta(x_3^L, C_{cl})}{n^{SL}(x_3^L, C_{cl})}. \quad (17)$$

From the data in Table 1, one finds that

$$\lambda = -0.34 \pm 0.01 \frac{\text{degree}}{\text{mol/m}^2}.$$

Thus, it appears that for the system considered, it is adsorption at the solid-liquid interface that controls the contact angle, and therefore γ^{SL} (see Eq. (11)).

For the results shown in Fig. 6, C_{cl} is fixed, but θ is seen to depend strongly on x_3^L . In Fig. 13 a sketch of a droplet on

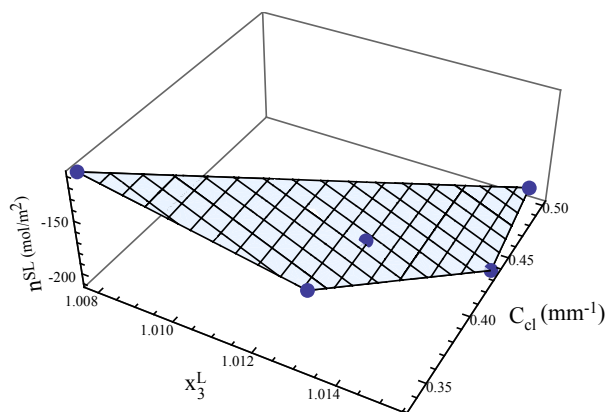


FIGURE 12. Three-dimensional plot n^{SL} as a function of x_3^L and C_{cl} for experiments described in Table 1.

an inclined solid surface in a gravity field is shown. It had been conventional to say that the contact angle hysteresis ($\theta_a > \theta_r$) resulted from surface roughness and surface heterogeneity underneath a droplet [18–21], until Gao and McCarthy [22] showed that contact angle hysteresis results from conditions at the three-phase line rather than from the conditions underneath the droplet. The results in this study give a mechanism supporting the conclusions of Gao and McCarthy [22].

Since θ has been found to depend on the properties at the three-phase line, x_3^L and C_{cl} , and because the magnitude of solid-liquid adsorption increases as x_3^L is increased, the results of this study indicate it is the conditions at different positions on the three-phase line that causes contact angle hysteresis for a droplet such as that shown in Fig. 13. And we may add that even on an absolutely smooth and homogeneous surface, the pressure in the liquid phase at the lower portion of the three-phase line would be greater than that at the higher portion. This pressure difference would give rise to contact angle hysteresis because x_3^L would be greater at the lower portion than at the upper portion of the three-phase line.

ACKNOWLEDGMENT

This work was supported by the Natural Sciences and Engineering Research Council of Canada, and the Canadian and European Space Agencies.

REFERENCES

- [1] Ward, C. A., and Wu, J., 2007. “Effect of adsorption on the surface tensions of solid-fluid interfaces”. *J. Phys. Chem. B*, **111**, pp. 3685–3694.
- [2] Ghasemi, H., and Ward, C. A., 2009. “Determination of the

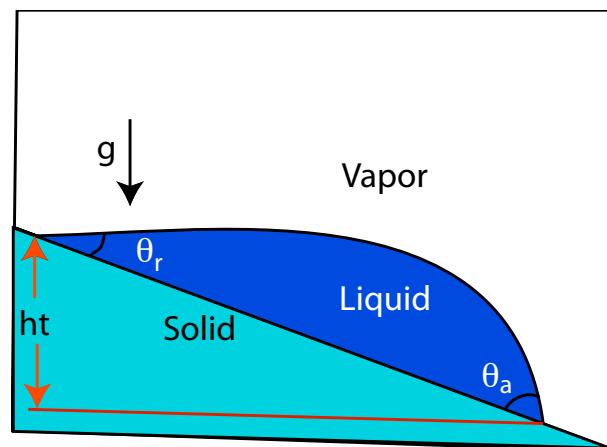


FIGURE 13. Three-dimensional plot n^{SL} as a function of x_3^L and C_{cl} for experiments described in Table 1.

surface tension of solids in the absence of adsorption”. *J. Phys. Chem. B*, **113**, pp. 12632–12634.

- [3] Ghasemi, H., and Ward, C. A., 2010. “Sessile-water-droplet contact angle dependence on adsorption at the solid-liquid interface”. *J. Phys. Chem. C*, **114**, pp. 5088–5100.
- [4] Brunauer, S., Emmett, P. H., and Teller, E., 1938. “Adsorption of gases in multimolecular layers”. *J. Am. Chem. Soc.*, **60**, pp. 309–319.
- [5] Frenkel, Y. I., 1946. *Kinetic Theory of Liquids*. Clarendon Press: Oxford, U.K.
- [6] Halsey, G., 1948. “Physical adsorption on non-uniform surfaces”. *J. Chem. Phys.*, **16**, p. 931.
- [7] Hill, T. L., 1952. “Theory of physical adsorption”. In *Advances in Catalysis and Related Subjects*, W. G. Frankenburg and V. I. Komarewsky, eds., Vol. 4. Academic Press: New York, p. 211.
- [8] Gibbs, J. W., 1961. “On the equilibrium of heterogeneous substances”. In *The Scientific Papers of J. Willard Gibbs*, H. A. Bumstead and R. G. V. Name, eds., Vol. 1. Dover, New York, pp. 55–349.
- [9] Wu, J., Farouk, T., and Ward, C. A., 2007. “Pressure dependence of the contact angle”. *J. Phys. Chem. B*, **111**, pp. 6189–6197.
- [10] Ward, C. A., Wu, J., and Keshavarz, A., 2008. “Measurement of the adsorption at solid-liquid interfaces from the pressure dependence of contact angles”. *J. Phys. Chem. B*, **112**, pp. 71–80.
- [11] Batchelor, G. K., 1967, pg. 20. *An Introduction to Fluid Dynamics*. Cambridge University Press, Cambridge.
- [12] Ward, C. A., and Sasges, M. R., 1998. “Effect of gravity on contact angle: A theoretical investigation”. *J. Chem. Phys.*, **109**, pp. 3651–3660.
- [13] de Gennes, P.-G., Brochard-Wyart, F., and Quéré, D., 2004.

Capillarity and Wetting Phenomena. Springer.

- [14] Seo, M., Sawamura, I., Grasjo, L., Haga, Y., and Sato, N., 1990. "Measurement of minute corrosion of copper thin film by a quartz crystal microbalance". *J. Soc. Material Science Japan*, **39**, pp. 357–361.
- [15] Matejova, L., Solcova, O., and Schneider, P., 2008. "Standard (master) isotherms of alumina, magnesia, titania and controlled-pore glass". *Microporous and Mesoporous Materials*, **107**, pp. 227–232.
- [16] Cejka, J., Zilkova, N., Rathousky, J., and Zukal, A., 2001. "Nitrogen adsorption study of organised mesoporous alumina". *Phys. Chem. Chem. Phys.*, **3**, pp. 5076–5081.
- [17] Ward, C. A., and Wu, J., 2008. "Effect of contact line curvature on solid-fluid surface tensions without line tension". *Phys. Rev. Lett.*, **100**, p. 256103.
- [18] Wenzel, R. N., 1936. "Resistance of solid surfaces to wetting by water". *Indust. Engin. Chem.*, **28**, p. 994.
- [19] Cassie, A. B. D., and Baxter, S., 1944. "Wettability of porous surfaces". *Trans. Faraday Soc.*, **40**, p. 546.
- [20] Hiemenz, P. C., 1977. *Principles of colloid and surface chemistry*. Marcel Dekker Inc.: New York.
- [21] Long, J., and Chen, P., 2006. "On the role of energy barriers in determining contact angle hysteresis". *Adv. Colloid Interface Sci.*, **127**, pp. 55–66.
- [22] Gao, L., and McCarthy, T., 2007. "How wenzel and cassie were wrong". *Langmuir*, **23**, pp. 3762–3765.